membranes

MDPI

Article

Evaluation of the Specific Energy Consumption of Sea Water Reverse Osmosis Integrated with Membrane Distillation and Pressure–Retarded Osmosis Processes with Theoretical Models

Shao-Chi Tsai [1], Wei-Zhi Huang [2,3], Geng-Sheng Lin [2,4], Zhen Wang [2,4], Kuo-Lun Tung [2,3,4,*] and Ching-Jung Chuang [1,*]

[1] R&D Center for Membrane Technology, Department of Chemical Engineering, Chung Yuan Christian University, Taoyuan 320, Taiwan; angela10221248@gmail.com
[2] Department of Chemical Engineering, National Taiwan University, Taipei 106, Taiwan; r07524009@g.ntu.edu.tw (W.-Z.H.); r05524113@ntu.edu.tw (G.-S.L.); d07524021@ntu.edu.tw (Z.W.)
[3] Water Innovation, Low Carbon and Environmental Sustainability Research Center (WInnER), National Taiwan University, Taipei 106, Taiwan
[4] Advanced Research Center for Green Materials Science and Technology, National Taiwan University, Taipei 106, Taiwan
* Correspondence: kltung@ntu.edu.tw (K.-L.T.); cjchuang@cycu.edu.tw (C.-J.C.); Tel.: +886-2-3366-3027 (K.-L.T.); +886-3265-4114 (C.-J.C.); Fax: +886-2-2362-3040 (K.-L.T.)

Abstract: In this study, theoretical models for specific energy consumption (SEC) were established for water recovery in different integrated processes, such as RO-PRO, RO-MD and RO-MD-PRO. Our models can evaluate SEC under different water recovery conditions and for various proportions of supplied waste heat. Simulation results showed that SEC in RO increases with the water recovery rate when the rate is greater than 30%. For the RO-PRO process, the SEC also increases with the water recovery rate when the rate is higher than 38%, but an opposite trend can be observed at lower water recovery rates. If sufficient waste heat is available as the heat source for MD, the integration of MD with the RO or RO-PRO process can significantly reduce SEC. If the total water recovery rate is 50% and MD accounts for 10% of the recovery when sufficient waste heat is available, the SEC values of RO, RO-PRO, RO-MD and RO-MD-PRO are found to be 2.28, 1.47, 1.75 and 0.67 kWh/m^3, respectively. These critical analyses provide a road map for the future development of process integration for desalination.

Keywords: reverse osmosis; pressure-retarded osmosis; membrane distillation; process integration; specific energy consumption

Citation: Tsai, S.-C.; Huang, W.-Z.; Lin, G.-S.; Wang, Z.; Tung, K.-L.; Chuang, C.-J. Evaluation of the Specific Energy Consumption of Sea Water Reverse Osmosis Integrated with Membrane Distillation and Pressure–Retarded Osmosis Processes with Theoretical Models. *Membranes* **2022**, *12*, 432. https://doi.org/10.3390/membranes12040432

Academic Editors: Pei Sean Goh, Takeshi Matsuura and Mohd Hafiz Dzarfan Othman

Received: 21 March 2022
Accepted: 13 April 2022
Published: 16 April 2022

1. Introduction

Climate change and water scarcity are the two pervasive problems posing serious threats to people around the world [1]. To solve these problems, seawater desalination technology for potable water has been rapidly developed. Reverse osmosis (RO) is currently the most common membrane process for desalination since high-performance RO membranes and modules have been well established. However, this process requires high electric energy consumption and the discharge of concentrated brine solution, which have confined the application of RO systems for years [2–7]. Thus, developing methods to reduce RO energy consumption and brine disposal is crucial for process efficiency and sustainability. One of the techniques that has received extensive attention is process integration, or the combination of RO with pressure-retarded osmosis (PRO) and/or membrane distillation (MD). This integrated approach can reduce the energy requirement for water recovery and enhance the water recovery rate [8].

PRO is an energy-harvesting process that converts the osmotic pressure of a saline solution to hydraulic pressure. In a PRO system, water from a low-salinity solution

(i.e., the feed solution, FS) is transported through the membrane to a high-salinity solution (i.e., the draw solution). This chemical potential difference can later be converted to electrical energy through hydroturbines [9–12] or mechanical energy through a pressure exchanger (PX). Additionally, MD is a promising technology for treating saline water and wastewater with high rejection factors. In an MD system, vapor molecules are transferred through a microporous hydrophobic membrane, and this process is driven by the partial vapor pressure difference induced by the temperature gradient across the membrane. This system relies on a thermally driven separation process; therefore, its performance is less sensitive to the salt concentration in the feed than the RO process [13–18].

Currently, there are five prevailing process integration schemes for desalination. The first is the simple RO process. Although it can produce potable water, most of the pressure energy leaves the membrane module with the brine. The second is the RO process combined with energy recovery devices (ERDs), such as PXs [19–21]. This process is designed to recover the residual energy of the brine. The third is the RO-PRO process [5,22,23]. This process can significantly reduce specific energy consumption (SEC) in the RO process. In this process, seawater flows into the RO system and is separated into pure water and brine. The RO brine is the input into the PRO system as the DS, which is later diluted, where energy is generated. The diluted brine stream from PRO can be discharged into the ocean without the concern of deteriorating marine habitats. The fourth approach is the RO-MD process. This process can increase water recovery [24]. The final method is the RO-MD-PRO process. This process can not only reduce SEC but can also increase water recovery [25].

To date, several research groups have evaluated the feasibility of integrating RO, MD, and PRO processes with software simulations. Prante et al. investigated RO and RO-PRO systems at a 50% RO water recovery rate. Their simulation results indicated that the SECs of RO and RO-PRO are 2.0 and 1.2 kWh/m^3, respectively, i.e., a 40% SEC reduction is achieved after RO is integrated with PRO [26]. Wan et al. studied models of RO without PX, RO with PX, and RO-PX-PRO systems. The results showed that when the RO water recovery rate is 25%, the SECs of these three systems are 5.51, 1.79, and 1.08 kWh/m^3, respectively; moreover, when the RO water recovery rate is increased to 50%, the SECs of these three systems is 4.13, 2.27, and 1.14 kWh/m^3, respectively [27]. Kim et al. discussed the SEC of RO and the RO-MD-PRO system, and they found that the SEC is 1.914 kWh/m^3 for RO with a water recovery rate of 49.7% and 1.61 kW/m^3 for RO-MD systems if (i) a heat source is supplied by waste heat and (ii) the MD water recovery rate is 5% [25]. Moreover, Ruiz-Garcia et al. analyzed the effect of different feed spacer geometries on the SWRO spiral-wounded membrane module. Their simulation results indicated that the longer the pressure vessel, the higher the influence of the feed spacer geometry on SEC [28].

Previous studies indicated that after integrating RO with MD and/or PRO, SEC can be reduced; however, these studies mainly focused on situations with specific RO and MD water recovery rates. It is acknowledged that (i) the water recovery rate is the main parameter that determines the minimum operating pressure of an RO system; (ii) the MD water recovery rate and percentage of waste heat from the heat source in the MD system affect the required operating energy; and (iii) the total water recovery of the integrated process affects the feed concentration of the PRO draw solution, which in turn affects the maximum power density generated by the PRO system. Therefore, the water recovery rate of RO and MD and the proportion of waste heat for the MD heat source have a crucial influence on SEC in the integrated process. Herein, we established theoretical models based on energy consumption in fluid transport, fluid mechanical energy recovery, the MD thermal energy demand and PRO energy production to analyze the SEC of RO, RO-PRO, RO-MD and RO-MD-PRO systems at different water recovery rates and different percentages of waste heat supplied for the MD system.

2. Materials and Methods

In this study, Equation (1) is used to indicate the energy consumed per unit of water production [2,3].

$$\text{SEC} = \frac{\text{power consumption (kW)}}{\text{water production rate } (\frac{\text{m}^3}{\text{h}})} \quad (1)$$

This study integrated RO with other unit operations, such as ERD, MD, and PRO, with the aim of analyzing SEC variations in different integrated processes.

2.1. SEC of the RO Process

A schematic diagram of the stand-alone RO process is shown in Figure 1. Since the suspended particles, microbes, and organic and inorganic matter in seawater can block the RO membrane and lead to fouling, the raw seawater feed solution is often pretreated with UF/MF prior to RO. The SEC for pretreatment per unit of RO permeate (SEC_{Pre}) is described in Equation (2).

$$SEC_{Pre} = \frac{SEC_{pre,sw} Q_{SW}}{Q_{P,RO}} = \frac{SEC_{pre,sw}}{Y_r} \quad (2)$$

where $SEC_{Pre,sw}$ is the pretreatment energy consumption per unit seawater feed solution, Q_{SW} is the volumetric flow rate of the seawater feed solution (m^3/h), $Q_{P,RO}$ is the RO permeate flow rate (m^3/h), and $Y_r \left(= \frac{Q_{P,RO}}{Q_{SW}}\right)$ is the RO water recovery rate.

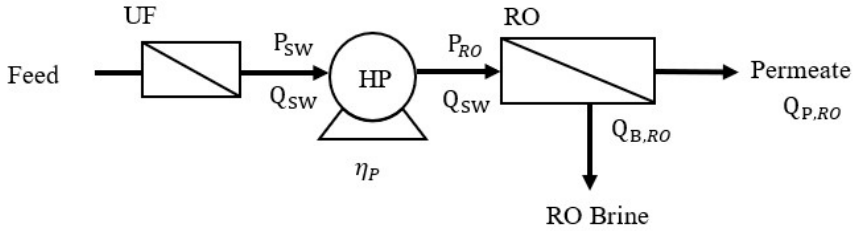

Figure 1. Schematic of the stand-alone RO process.

Glueckstern and Priel suggested that when ultrafiltration is used prior to RO, $SEC_{Pre,sw}$ is 0.095 kWh/m^3 [29]. Pretreated seawater is pressurized via a high-pressure pump (HP) to the RO operating pressure (P_{RO}) and then enters the RO unit. The minimum operating pressure required for RO is the osmotic pressure of the brine. In this study, the RO operating condition is set equal to the minimum operating pressure at each water recovery rate (i.e., osmotic pressure of brine in RO) for determining the SEC. The SEC of the stand-alone RO process (SEC_{RO}) was evaluated by Equation (3) [2,3].

$$SEC_{RO} = \frac{\pi_{sw} R_t}{\eta_p Y_r (1 - Y_r)} \quad (3)$$

where π_{sw} is the osmotic pressure of the feed solution (bar), R_t is the salt rejection rate of the membrane, and η_p is the HP efficiency. The osmotic pressure can be calculated by the van 't Hoff equation as below [30]:

$$\pi = iCRT \quad (4)$$

where π is the osmotic pressure (bar), i is the van 't Hoff factor (i = 1.9 when the solute is NaCl [30]), C is the salt concentration (M), R is the ideal gas constant, and T is the temperature (K). In this study, the temperature is set to 298 K, unless a different value is specified.

The RO-ERD process is presented in Figure 2. ERD is utilized to recover the remaining mechanical energy in the brine solution; herein, a PX was selected as the ERD. After seawater pretreatment, part of the feed solution enters the RO unit via HP, and the other

part enters the RO unit via the PX and booster pump (BP). The brine solution is then discharged after the available brine energy is transferred via the PX at atmospheric pressure. The SEC of the RO-ERD process ($SEC_{RO\text{-}ERD}$) can be calculated as in Equation (5) [2,3]:

$$SEC_{RO\text{-}ERD} = \frac{\pi_{sw} R_t (1 - \eta_{PX}(1 - Y_r))}{\eta_p Y_r (1 - Y_r)} \quad (5)$$

where η_{PX} is the PX efficiency.

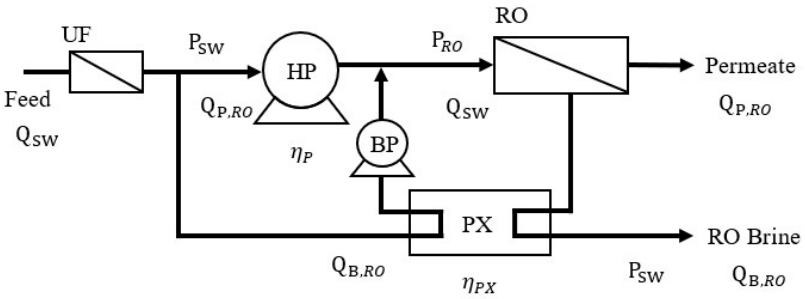

Figure 2. Schematic of RO with an energy recovery device (RO-ERD).

2.2. SEC of the RO-PRO Process

Figure 3 shows the flow chart of the RO-PRO process. The brine solution, which served as the DS for the PRO unit, is discharged from the RO system and releases pressure via the PX1 to PRO operating pressure (P_{PRO}). Previous studies often used low-saline water as the FS for PRO; however, in practice, urban wastewater should be considered as the PRO FS [27]. In this study, a 0.01-M NaCl solution is used to simulate the FS of the PRO unit. Considering the environmental impact after a large amount of brine discharge, the RO brine is assumed to be diluted to the original seawater concentration after passing through the PRO unit. The SEC of RO-PRO ($SEC_{RO\text{-}PRO}$) can be calculated as in Equation (6).

$$SEC_{RO\text{-}PRO} = \frac{\dot{W}_{pump,RO\text{-}PRO}}{\eta_p Q_{P,RO}} = \frac{\dot{W}_{pump,RO} - \dot{W}_{pump,PX1} - \dot{W}_{pump,PX2}}{\eta_p Q_{P,RO}} \quad (6)$$

where $\dot{W}_{pump,RO\text{-}PRO}$ and $\dot{W}_{pump,RO}$ are the energy consumption levels of the HP in RO-PRO and stand-alone RO processes, respectively. $\dot{W}_{pump,RO}$ can be calculated in Equation (7).

$$\dot{W}_{pump,RO} = P_{RO} \times Q_{SW} \quad (7)$$

$\dot{W}_{pump,PX1}$ is the mechanical energy recovered by PX1, $\dot{W}_{pump,PX2}$ is the energy recovered by PX2, PRO is the RO operating pressure, and Q_{sw} is the volumetric flow rate at the seawater inlet.

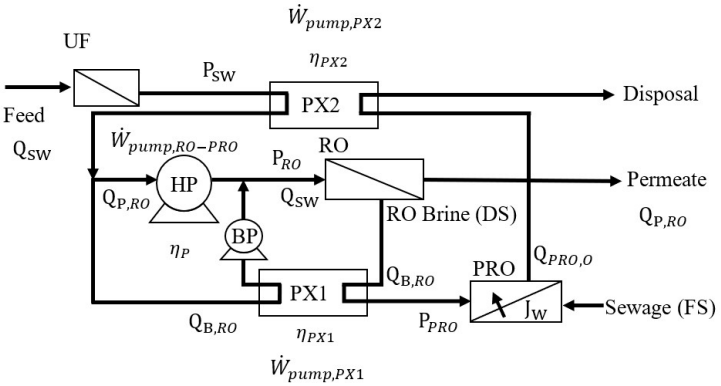

Figure 3. Schematic of the hybrid RO-PRO process.

Previous studies indicated that the maximum power density can be obtained when the operating pressure equals half of the transmembrane osmotic pressure [31]. Thus, P_{PRO} is set accordingly in Equation (8).

$$P_{PRO} = \frac{1}{2}(\pi_{RO\text{-}PRO,DS} - \pi_{PRO,FS}) \quad (8)$$

where $\pi_{RO-PRO,DS}$ and $\pi_{PRO,FS}$ are the osmotic pressures of the DS and FS, respectively. The recovery of the mechanical energy of the RO brine after depressurization from P_{RO} to P_{PRO} via PX1 ($\dot{W}_{pump,PX1}$) can be evaluated by Equation (9).

$$\dot{W}_{pump,PX1} = \eta_{PX}(P_{RO} - P_{PRO})Q_{B,RO} \quad (9)$$

where $Q_{B,RO}$ is the RO brine flow rate. The recovery of mechanical energy at the PRO DS outlet after depressurization from P_{PRO} to atmospheric pressure via PX2 ($\dot{W}_{pump,PX2}$) can be evaluated by Equation (10).

$$\dot{W}_{pump,PX2} = \eta_{PX}\left(P_{PRO} - 0\right)(Q_{B,RO} + Q_{P,PRO}) = \eta_{PX}P_{PRO}Q_{PRO,O} \quad (10)$$

where $Q_{PRO,O}$ and $Q_{P,PRO}$ are the flow rate at the PRO DS outlet and permeation rate through the PRO membrane, respectively. After combining Equation (6) and (10), the SEC of the RO-PRO process can be presented as shown in Equation (11).

$$SEC_{RO\text{-}PRO} = SEC_{RO\text{-}ERD} - \frac{\eta_{PX}P_{PRO}(Q_{P,PRO}/Q_{SW})}{\eta_p(Y_r)} \quad (11)$$

2.3. SEC of the RO-MD Process

Figure 4 illustrates the RO-MD process. RO brine is first depressurized to P_{MD} via PX3 and then transported to the MD unit. The SEC of RO-MD ($SEC_{RO\text{-}MD}$) and the mechanical energy recovered via PX3 ($\dot{W}_{pump,PX3}$) can be presented by Equations (12) and (13), respectively.

$$SEC_{RO\text{-}MD} = \frac{\dot{W}_{pump,RO\text{-}MD}}{\eta_p(Q_{P,RO} + Q_{P,MD})} = \frac{\dot{W}_{pump,RO} - \dot{W}_{pump,PX3}}{\eta_p(Q_{P,RO} + Q_{P,MD})} \quad (12)$$

$$\dot{W}_{pump,PX3} = \eta_{PX}(P_{RO} - P_{MD})Q_{B,RO} \quad (13)$$

where $Q_{P,MD}$ is the MD permeate flow rate and $Q_{B,MD}$ is the brine flow rate discharged from MD. Assuming there is sufficient waste heat for the MD unit, $SEC_{RO\text{-}MD}$ described in Equation (12) can be converted to the form shown in Equation (14).

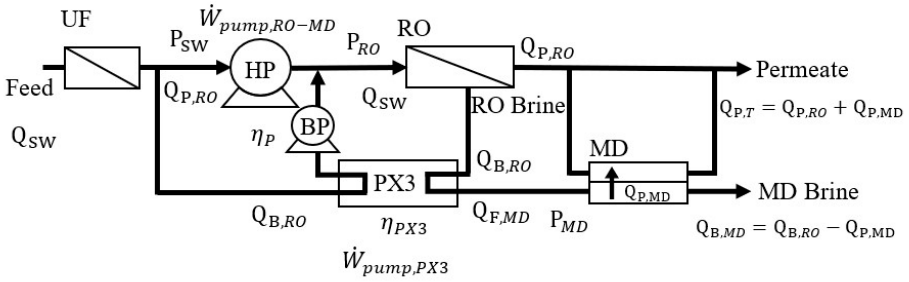

Figure 4. Schematic of the hybrid RO-MD process.

$$SEC_{RO\text{-}MD} = \frac{\pi_{sw}R_t(1 - \eta_{PX}(1 - Y_r)) + \eta_{PX}P_{MD}(1 - Y_r)^2}{\eta_p(1 - Y_r)(Y_r + Y_m)} \quad (14)$$

where $Y_m \left(= \frac{Q_{P,MD}}{Q_{SW}}\right)$ is the MD water recovery rate. If the waste heat supply for MD is not sufficient and a supplementary heat source is then required, the MD thermal energy consumption ($SEC_{Thermal\text{-}MD}$) and total SEC of RO-MD ($SEC_{RO\text{-}MD}^{Thermal}$) can be expressed as shown in Equations (15) and (16).

$$SEC_{Thermal\text{-}MD} = (1 - X)\frac{\rho_{P,MD} Q_{P,MD} \Delta H_{vap}}{EE\left(Q_{P,RO} + Q_{P,MD}\right)} \quad (15)$$

$$SEC_{RO\text{-}MD}^{Thermal} = SEC_{RO\text{-}MD} + SEC_{Thermal\text{-}MD} \quad (16)$$

where X is the proportion of waste heat supplied to the total thermal energy consumption of MD and EE is the energy efficiency of MD, which is defined as the percentage of the thermal energy associated with liquid evaporation [13]. $\rho_{P,MD}$ is the density of water, and ΔH_{vap} is the enthalpy of vaporization.

2.4. SEC of the RO-MD-PRO Process

The power density of PRO can be enhanced by increasing the DS concentration; therefore, utilizing the high-concentration RO-MD brine discharge as the PRO DS can improve power production. Figure 5 is the schematic diagram of the integrated RO-MD-PRO process. MD brine is pressurized in the PRO unit as the DS. It is assumed that PRO DS will be diluted to the initial seawater concentration and that the mechanical energy will be transferred to the RO feed solution via PX5. The SEC of RO-MD-PRO ($SEC_{RO\text{-}MD\text{-}PRO}$) and the recovery mechanical energy from PX4 ($\dot{W}_{pump,PX4-recover}$) can be expressed as shown in Equations (17) and (18).

$$SEC_{RO\text{-}MD\text{-}PRO} = \frac{\dot{W}_{pump,ROMD\text{-}PRO}}{\eta_p\left(Q_{P,RO} + Q_{P,MD}\right)} = \frac{\dot{W}_{pump,RO} - \dot{W}_{pump,PX4\text{-}recover} + \dot{W}_{pump,PX4\text{-}reuse} - \dot{W}_{pump,PX5}}{\eta_p\left(Q_{P,RO} + Q_{P,MD}\right)} \quad (17)$$

$$\dot{W}_{pump,PX4\text{-}recover} = \eta_{PX}\left(P_{RO} - P_{MD}\right)Q_{B,RO} \quad (18)$$

$$\dot{W}_{pump,PX4\text{-}reuse} = \eta_{PX}\left(P_{PRO} - P_{MD}\right)Q_{B,MD} \quad (19)$$

$$\dot{W}_{pump,PX5} = \eta_{PX}\left(P_{PRO} - 0\right)\left(Q_{B,MD} + Q_{P,PRO}\right) \quad (20)$$

where $\dot{W}_{pump,PX4\text{-}reuse}$ is the mechanical energy transferred from the RO brine to PRO DS via PX4, and $\dot{W}_{pump,PX5}$ is the mechanical energy recovered from the PRO DS outlet as the DS depressurized from PPRO to atmospheric pressure via PX5.

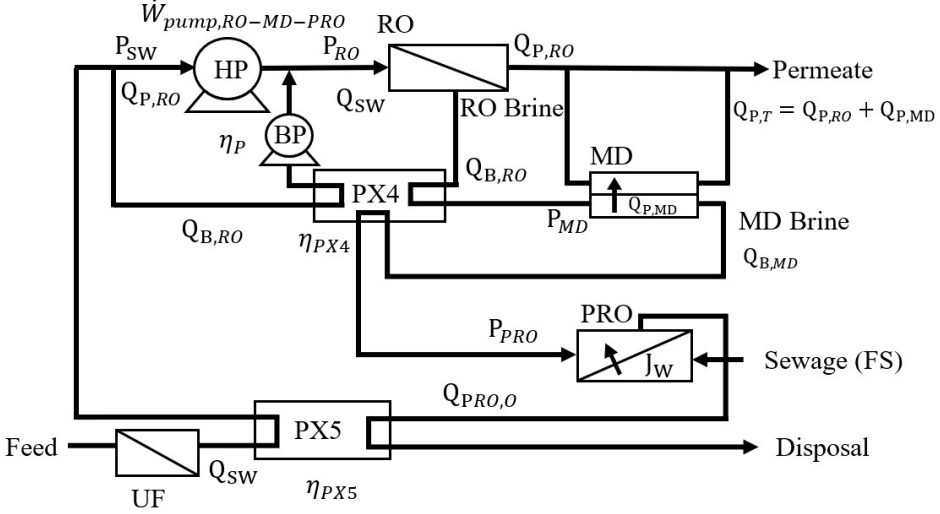

Figure 5. Schematic of the hybrid RO-MD-PRO process.

By combining Equations (17)–(20) and assuming that there is sufficient waste heat to meet the thermal energy requirement of MD (X = 1), the SEC of the RO-MD-PRO process can be obtained.

$$SEC_{RO\text{-}MD\text{-}PRO}(X=1) = \frac{\pi_{sw} R_t (1-\eta_{PX}(1-Y_r))}{\eta_p (1-Y_r)(Y_r+Y_m)} + \frac{\eta_{PX} P_{MD} Y_m - \eta_{PX} P_{PRO}(Q_{P,PRO}/Q_{SW})}{\eta_p (Y_r+Y_m)} \quad (21)$$

2.5. The Fractional Energy Savings

Based on the RO-ERD process, the fractional energy savings (FES) in water production based on hybrid processes can be defined as shown in Equation (22).

$$FES = \frac{SEC_{RO\text{-}ERD} - SEC_{integrated\ process}}{SEC_{RO\text{-}ERD}} \times 100\% \quad (22)$$

When $SEC_{integrated\ process}$ is zero, the FES equals 100%. Under these circumstances, energy consumption and energy generation are equal, i.e., no further energy supply is required for this process. However, when the FES is greater than 100%, the energy generation is larger than the energy consumption, and $SEC_{integrated\ process}$ for this process is negative, and vice versa.

3. Results and Discussion

Herein, the SEC of RO, RO-PRO, RO-MD, and RO-MD-PRO were analyzed under different operating conditions. These calculated SECs were further compared with data from previous research articles.

3.1. RO Process

Table 1 lists the parameters used in stand-alone RO and/or RO-ERD process simulations. Figure 6 shows the variations in SEC_{RO} and $SEC_{RO\text{-}ERD}$ at different water recovery rates. The SEC of the pretreatment unit, SEC_{pre}, is also shown in Figure 6. As the water recovery rate decreases, the amount of seawater to be pretreated increases, which leads to an increase in SEC_{pre}. SEC_{RO} is much higher than SEC_{pre}; therefore, the influence of SEC_{pre} on SEC is small in the stand-alone RO process. The SEC_{RO} reaches a minimum value of 4.0 kWh/m^3 when the water recovery rate is 51%. Additionally, $SEC_{RO\text{-}ERD}$ is lower than SEC_{RO}; hence, the addition of the pretreatment unit has a pronounced influence on the total SEC. In the RO-ERD process, SEC is maintained at approximately 2.0 kWh/m^3 when the water recovery rate ranges from 27–36%.

Table 1. The parameters used in stand-alone RO and/or RO-ERD process simulations.

C_{SW}	Seawater salt concentration (M)	0.589
R_t	Salt rejection percentage of the membrane (-)	99%
η_p	RO pump efficiency (-)	80%
η_{PX}	Pressure exchanger efficiency (-)	95%
$Q_{P,RO}$	The volumetric flowrate of RO permeate(m^3/day)	100,000

3.2. RO-PRO Process

The PRO unit provides both power generation and a reduction in the brine discharge concentration. Figure 7 shows the energy consumption of RO and energy generation of PRO in the RO-PRO process. When the water recovery rate is higher than 29%, both power generation and energy consumption increase as the recovery rate increases; however, the rate of increase of the latter is significantly larger. The results show that RO energy consumption is more dominant than PRO energy generation in the RO-PRO process.

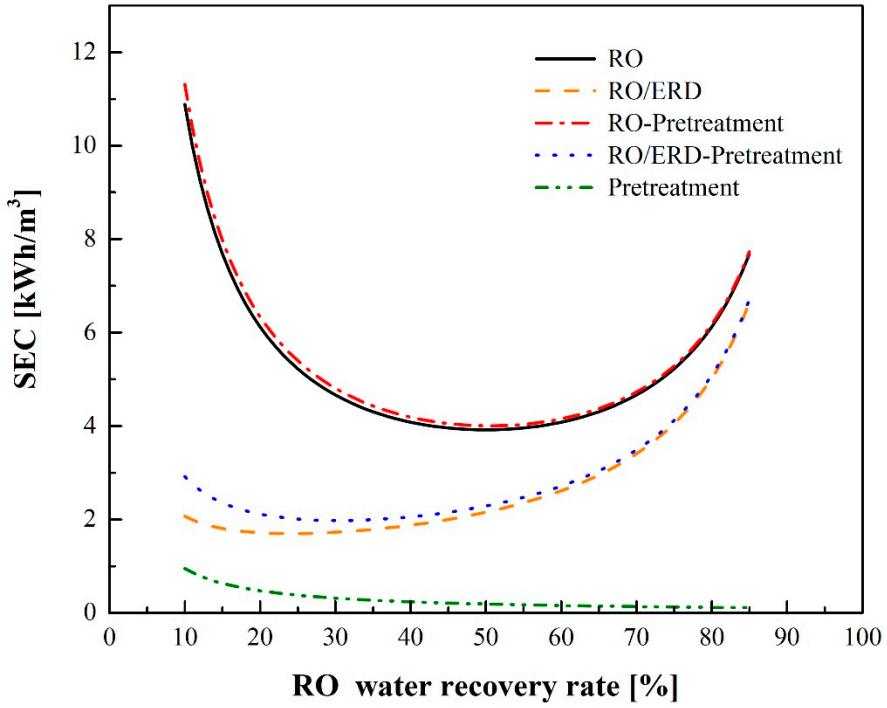

Figure 6. Comparison of SEC between the stand-alone RO and RO-ERD processes simulated with and without pretreatment.

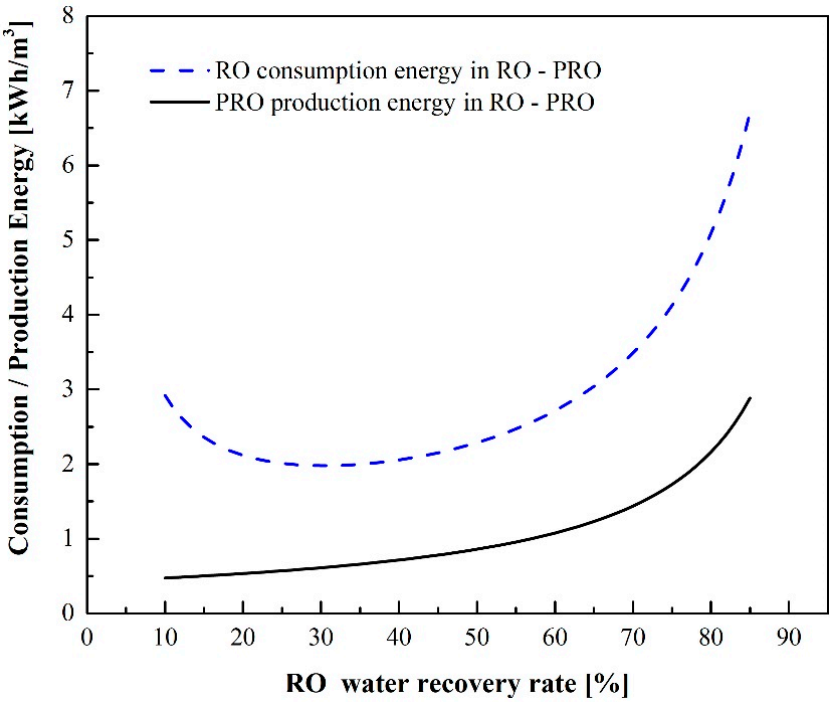

Figure 7. Comparison of RO energy consumption and PRO energy production in the RO-PRO process.

Figure 8 shows a comparison of SEC between the RO-ERD and RO-PRO processes. When the water recovery rate is low, the SEC of these two processes decreases as the water recovery rate increases. Notably, the increased water recovery rate will reduce the amount of seawater required, thereby decreasing SEC_{pre}. However, when the water recovery rate is high, SEC increases as the water recovery rate increases. Since the RO operating pressure increases as the water recovery rate increases, HP energy consumption results in

an increase in the total SEC. When the RO water recovery rate is 30%, the RO-ERD process yields a minimum SEC of 1.97 kWh/m^3, and the RO-PRO process has a minimum SEC of 1.33 kWh/m^3 when the RO water recovery rate is 38% [32]. Comparing the two processes, RO-PRO has a lower SEC due to the energy generation by PRO and obtains a higher water recovery rate at the minimum SEC.

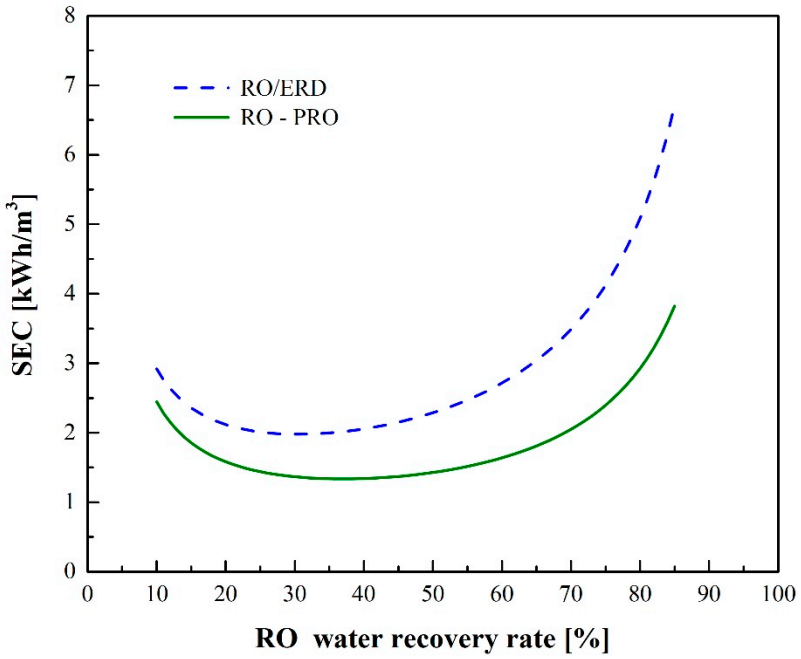

Figure 8. Simulation results of SE for CRO-ERD and RO-PRO at different water recovery rates.

3.3. RO-MD Process

In the RO-MD process, MD can enhance the overall water recovery rate. This section will discuss the operating parameters associated with the minimum SEC and the influence of the heat source for the MD unit on SEC. Table 2 lists the parameters of the simulation. Since the RO water recovery rate (Y_r) is lower than 50%, Y_r is set to 40% or 50% in the simulation. Considering the saturated concentration of NaCl, the overall water recovery rate ($Y_r + Y_m$) of seawater in the integrated process should be less than 85%. Moreover, the liquid entry pressure (LEP) of the MD membrane should also be taken into consideration; thus, the MD operating pressure is set to 3 bar [33]. For the estimation of the MD heat requirement, EE is set to 60% [27].

Table 2. Parameters for RO-MD process simulations.

Y_r	RO water recovery rate (-)	40%, 50%
Y_m	MD water recovery rate (-)	1~45%, 1~35%
Y_t	Total water recovery rate (-)	≤85%
P_{MD}	MD pressure [4]	3
ΔH_{vap}	Enthalpy of vaporization (kJ/kg)	2382
EE	Energy efficiency of MD (-)	60%
T_{FMD}	Temperature of the MD feed solution (°C)	70
T_{BRO}	Temperature of the RO brine (°C)	30

Figure 9 displays the $SEC_{RO\text{-}MD}$ values at different water recovery rates. When the RO water recovery rate remains constant and there is sufficient waste heat as the MD heat source (Equation (15), X = 1), $SEC_{RO\text{-}MD}$ can be reduced as the MD water recovery rate increases. When the MD water recovery rate increases from 1% to 45%, $SEC_{RO\text{-}MD}$ decreases from 2.14 to 1.03 kWh/m^3. If no waste heat supplies the MD process, SEC will

largely increase as the water recovery rate increases due to the high energy consumption of the enthalpy of vaporization from the MD process. When the RO recovery rate is maintained at 40% and the MD water recovery rate is 45%, $SEC_{RO\text{-}MD}$ can be as high as 584 kWh/m^3. Because the amount of waste heat supplied by industrial sites is confined, the water recovered by the MD unit in large-scale seawater operations is less than 10% of all water recovered. Thus, both the gray and blue rectangular areas in Figure 9 reflect practical conditions.

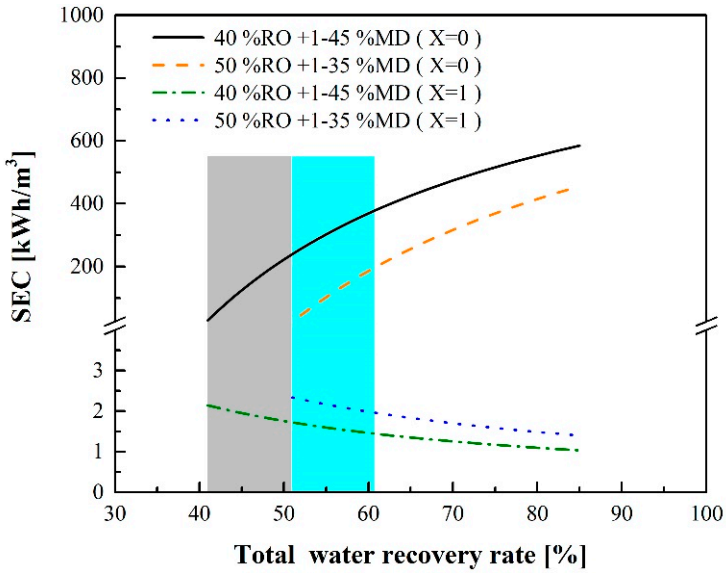

Figure 9. SEC of the RO-MD process with or without waste heat contribution.

Figure 9 indicates that waste heat can largely influence $SEC_{RO\text{-}MD}$. If there is not sufficient waste heat supply, electricity, steam or other heat sources should be provided for the MD process. Figure 10 shows the relationship between the total water recovery rate and $SEC_{RO\text{-}MD}$ at different percentages of the waste heat supply when the RO water recovery rate is 40%. If the waste heat could provide 90% or 95% of the required heating energy (X = 0.9 or 0.95), $SEC_{RO\text{-}MD}$ could be reduced to 25.5 or 13.61 kWh/m^3, respectively, when the total water recovery rate is 51%.

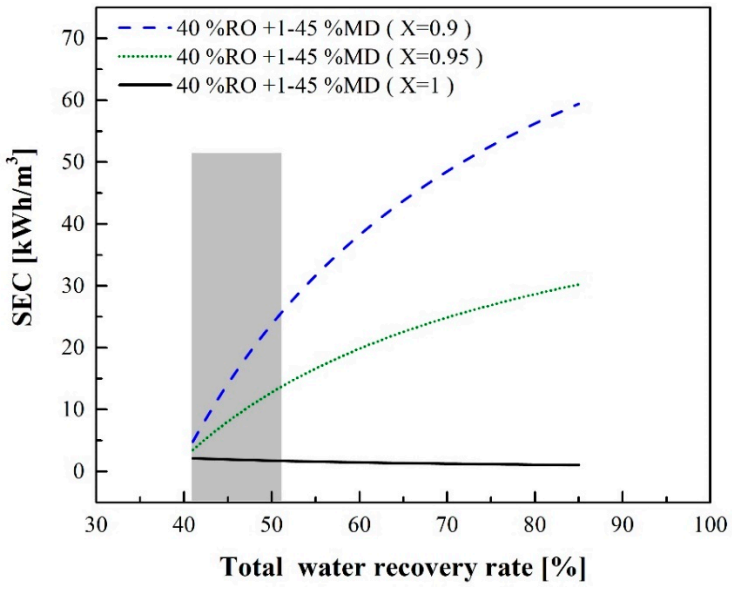

Figure 10. SEC of the RO-MD process with or without a sufficient waste heat source for MD.

3.4. RO-MD-PRO Process

Figure 11 displays an SEC comparison between the RO-MD-PRO and RO-PRO processes. It is assumed that there is sufficient waste heat supply for MD operations. The straight line indicates $SEC_{RO\text{-}MD\text{-}PRO}$ at different water recovery rates. This figure also displays $SEC_{RO\text{-}ERD}$ and $SEC_{RO\text{-}PRO}$ when the RO water recovery rate is 40%. When the RO water recovery rate is held constant, $SEC_{RO\text{-}MD\text{-}PRO}$ decreases as the MD water recovery rate increases. Moreover, when the total water recovery rate is 64%, $SEC_{RO\text{-}MD\text{-}PRO}$ changes from positive to negative, which suggests that energy generation by PRO is larger than energy consumption by pumping.

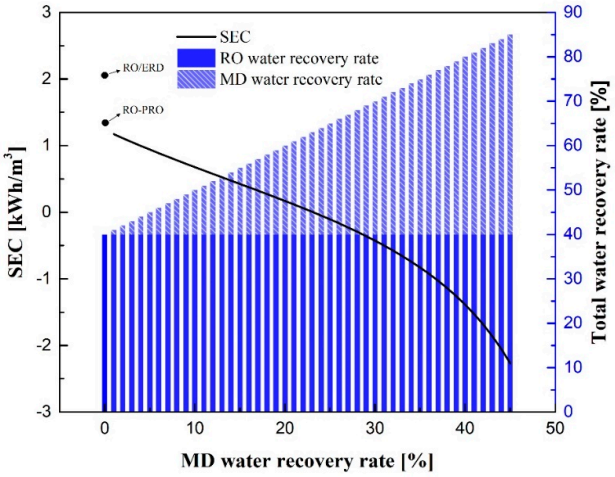

Figure 11. SEC of the RO-MD-PRO process at various MD water recovery rates and total water recovery rates.

3.5. The Fractional Energy Savings(FES) of Integrated Processes

Figure 12 illustrates the FES for different water recovery rates. When the MD heat requirement is totally met by waste heat, the FES of RO-MD, RO-PRO, and RO-MD-PRO increases as the total water recovery rate increases since MD can enhance water recovery and PRO can extract osmotic pressure energy from brine discharge. At the same water production rate, when the water recovery rate increases, the amount of brine will decrease, but the brine concentration will increase. According to Equations (7) and (9), these two phenomena have opposite effects on PRO energy generation. Therefore, the increase in the rate of FES for RO-PRO is lower than that for RO-MD and RO-MD-PRO.

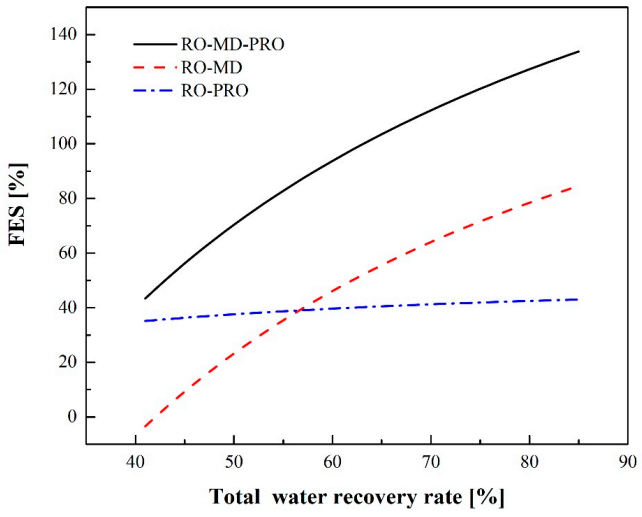

Figure 12. FES for different integrated processes.

3.6. Comparison with RO-Integrated Processes in the Literature

Table 3 lists the SEC values of RO-integrated processes reported in previous studies and in this study. The results indicate that previous studies mainly focused on SEC at specific water recovery rates, and few have evaluated the impact of the MD water recovery rate on SEC. In this study, SEC at a total water recovery rate ranging from 10% to 85% was studied; moreover, the conditions associated with different MD water recovery rates were discussed. Thus, this work can provide a broader range of evaluations for process integration. Compared with Wan and Chung's results [27], $SEC_{RO\text{-}PRO}$ in this work is slightly higher than theirs (0.28 kWh/m^3) when the RO water recovery rate is 50%. This difference is mainly attributed to the different efficiency settings of the pump and PX. Compared with the work of Kim et al. [25], $SEC_{RO\text{-}MD\text{-}PRO}$ in this study is lower. The difference is that this study assumes that the MD heat source is completely provided by waste heat. When the ratio of MD water recovery to total water recovery increases, the SEC of the RO-MD-PRO process can be reduced.

Table 3. SEC values from the literature and simulation results in this study.

RO Process	RO-PRO Process	RO-MD Process	RO-MD-PRO Process	Ref
Y_r = 20, 30% SEC = 3.73, 3.38 kWh/m^3	Y_r = 20, 30% SEC = 3.08, 2.64 kWh/m^3			[34]
Y_r = 50% SEC = 2 kWh/m^3	Y_r = 50% SEC = 1.2 kWh/m^3			[26]
Y_r = 25, 50% SEC = 1.79, 2.27 kWh/m^3	Y_r = 25, 50% SEC = 1.08, 1.14 kWh/m^3			[27]
Y_r = 50% SEC = 1.91 kWh/m^3	Y_r = 50% SEC = 1.78 kWh/m^3		Y_r = 50%, Y_m =2% SEC = 1.60 kWh/m^3	[25]
SEC = 3.32 kWh/m^3	SEC = 2.869 kWh/m^3	SEC = 2.809 kWh/m^3	SEC = 2.683 kWh/m^3	[35]
Y_r = 10 ~ 85% SEC = 1.91 ~ 8 kWh/m^3	Y_r = 10 ~ 85% SEC = 1.33 ~ 4 kWh/m^3	Y_r = 10 ~ 85% SEC = 1.03 ~ 2.28 kWh/m^3	Y_r = 10 ~ 85% SEC = 0 ~ 1.33 kWh/m^3	This work

4. Conclusions

Based on the principles of energy consumption during fluid transport, fluid mechanical energy recovery, MD thermal energy demand and PRO energy generation, this study established theoretical SEC models for water recovery by integrating RO with other unit operations, such as MD and PRO. The purpose of this study was to analyze the effect of the total water recovery rate on SEC in different integrated processes, such as RO-PRO, RO-MD and RO-MD-PRO. From this study, the following conclusions can be drawn.

(1) The brine flow rate decreases as RO water recovery increases. When the water recovery rate is greater than 30%, recyclable mechanical energy in the PX begins decreasing in availability, and SEC starts increasing. The minimum SEC is 1.97 kWh/m^3 at a recovery rate of 30% for the RO/ERD process.

(2) For the RO-PRO process, SEC reaches a minimum value of 1.33 kWh/m^3 at a recovery rate of 38%. RO-PRO can give a lower SEC than RO due to the energy generation by PRO, and a higher water recovery rate is obtained at the minimum SEC.

(3) For the RO-MD process, when the RO water recovery rate remains constant and there is sufficient waste heat as the MD heat source, SEC can be reduced as the MD water recovery rate increases. If the water recovery rate of RO is fixed at 40% and the total water recovery rate is 85%, SEC is 1.03 kWh/m^3.

(4) For the RO-MD-PRO process and an RO water recovery rate that is constant at 40%, the energy consumption due to pumping and energy generation by PRO reaches a balance at a total water recovery rate of 64%, which means that SEC is zero under these conditions. When the total recovery rate exceeds 64%, the FES of the integrated process is greater than 100%.

(5) The limit of the water recovery rate for SWRO is generally 50%. Thus, if we assume that the RO water recovery rate is 50%, the recovery rate of water for MD is 10%, and sufficient waste heat is available as a heat source for the MD unit; the SECs of the RO, RO-PRO, RO-MD and RO-MD-PRO processes are found to be 2.28, 1.47, 1.75, and 0.67 kWh/m^3, respectively. The corresponding FES values of the integrated processes are 37%, 23% and 70% when compared with the baseline RO process.

It is noted that this study only evaluated the energy consumption for water production from integrated RO processes. When evaluating the water production cost in future engineering applications, further consideration of capital costs, such as land, construction, equipment, module, maintenance and operation costs, is needed.

Author Contributions: Conceptualization, S.-C.T. and C.-J.C.; validation, Z.W. and K.-L.T.; investigation, S.-C.T., W.-Z.H., G.-S.L., Z.W., K.-L.T. and C.-J.C.; writing—original draft preparation, S.-C.T., W.-Z.H., G.-S.L., K.-L.T. and C.-J.C.; writing—review and editing, Z.W. and K.-L.T.; visualization, K.-L.T. and C.-J.C.; supervision, K.-L.T. and C.-J.C. All authors have read and agreed to the published version of the manuscript.

Funding: The water Resource Agency, Ministry of Economic Affairs, Taiwan for the financial support (Project number: MOEAWRA1080341). The Ministry of Science and Technology (MOST) in Taiwan (Project number: 109-2221-E-002-102-MY3, 110-2622-E-002-014 and 111-2634-F-002-016), and "Advanced Research Center of Green Materials Science and Technology" (111L891801) from The Feature Area Research Center Program within the framework of the Higher Education Sprout Project by the Ministry of Education (MOE), Taiwan (111L9006).

Institutional Review Board Statement: Not applicable.

Informed Consent Statement: Informed consent was obtained from all subjects involved in the study.

Data Availability Statement: Data associated with this research are mentioned in the article.

Conflicts of Interest: The authors declare no conflict of interest.

Abbreviations

The following abbreviations are used in this manuscript:

Nomenclature

BP	Booster pump
C	Salt concentration
DS	Draw solution
EE	Energy efficiency
ERDs	Energy recovery devices
FES	Fractional energy savings
FS	Feed solution
HP	High-pressure pump
MD	Membrane distillation
P	Pressure
PRO	Pressure–retarded osmosis
PX	Pressure exchanger
Q	Volumetric flowrate
RO	Reverse osmosis
R_t	Salt rejection rate
SEC	Specific energy consumption
SW	Seawater
T	Temperature
Y	Water recovery rate

Greek letters	
ρ	Density of water
π	Osmotic pressure of the feed solution
η	Efficiency
ΔH	Enthalpy
Subscripts	
p	RO pump
pre	Pretreatment unit
r	RO
m	MD
t	Total
vap	Vaporization
FMD	MD feed solution
BRO	RO brine

References

1. Guirguis, M.J. *Energy Recovery Devices in Seawater Reverse Osmosis Desalination Plants with Emphasis on Efficiency and Economical Analysis of Isobaric versus Centrifugal Devices*; University of South Florida: Tampa, FL, USA, 2011.
2. Zhu, A.; Christofides, P.D.; Cohen, Y. Minimization of energy consumption for a two-pass membrane desalination: Effect of energy recovery, membrane rejection and retentate recycling. *J. Membr. Sci.* **2009**, *339*, 126–137. [CrossRef]
3. Zhu, A.; Christofides, P.D.; Cohen, Y. Effect of thermodynamic restriction on energy cost optimization of RO membrane water desalination. *Ind. Eng. Chem. Res.* **2009**, *48*, 6010–6021. [CrossRef]
4. Altaee, A.; Millar, G.J.; Zaragoza, G. Integration and optimization of pressure retarded osmosis with reverse osmosis for power generation and high efficiency desalination. *Energy* **2016**, *103*, 110–118. [CrossRef]
5. Sakai, H.; Ueyama, T.; Irie, M.; Matsuyama, K.; Tanioka, A.; Saito, K.; Kumano, A. Energy recovery by PRO in sea water desalination plant. *Desalination* **2016**, *389*, 52–57. [CrossRef]
6. Basile, A.; Cassano, A.; Rastogi, N.K. *Advances in Membrane Technologies for Water Treatment: Materials, Processes and Applications*; Elsevier: Amsterdam, The Netherlands, 2015.
7. Sauvet-Goichon, B. Ashkelon desalination plant—A successful challenge. *Desalination* **2007**, *203*, 75–81. [CrossRef]
8. Cheng, Z.L.; Han, G. Pressure Retarded Osmosis-Membrane Distillation. In *Membrane Distillation*; CRC Press: Boca Raton, FL, USA, 2019; pp. 285–300.
9. Achilli, A.; Cath, T.Y.; Childress, A.E. Power generation with pressure retarded osmosis: An experimental and theoretical investigation. *J. Membr. Sci.* **2009**, *343*, 42–52. [CrossRef]
10. Cheng, Z.L.; Li, X.; Chung, T.-S. The forward osmosis-pressure retarded osmosis (FO-PRO) hybrid system: A new process to mitigate membrane fouling for sustainable osmotic power generation. *J. Membr. Sci.* **2018**, *559*, 63–74. [CrossRef]
11. Chou, S.; Wang, R.; Shi, L.; She, Q.; Tang, C.; Fane, A.G. Thin-film composite hollow fiber membranes for pressure retarded osmosis (PRO) process with high power density. *J. Membr. Sci.* **2012**, *389*, 25–33. [CrossRef]
12. Gonzales, R.R.; Abdel-Wahab, A.; Adham, S.; Han, D.S.; Phuntsho, S.; Suwaileh, W.; Hilal, N.; Shon, H.K. Salinity gradient energy generation by pressure retarded osmosis: A review. *Desalination* **2021**, *500*, 114841. [CrossRef]
13. Ullah, R.; Khraisheh, M.; Esteves, R.J.; McLeskey, J.T., Jr.; AlGhouti, M.; Gad-el-Hak, M.; Tafreshi, H.V. Energy efficiency of direct contact membrane distillation. *Desalination* **2018**, *433*, 56–67. [CrossRef]
14. Lin, S.; Yip, N.Y.; Elimelech, M. Direct contact membrane distillation with heat recovery: Thermodynamic insights from module scale modeling. *J. Membr. Sci.* **2014**, *453*, 498–515. [CrossRef]
15. Lawson, K.W.; Lloyd, D.R. Membrane distillation. *J. Membr. Sci.* **1997**, *124*, 1–25. [CrossRef]
16. Phattaranawik, J.; Jiraratananon, R.; Fane, A.G. Heat transport and membrane distillation coefficients in direct contact membrane distillation. *J. Membr. Sci.* **2003**, *212*, 177–193. [CrossRef]
17. Bui, V.; Vu, L.T.; Nguyen, M.H. Modelling the simultaneous heat and mass transfer of direct contact membrane distillation in hollow fibre modules. *J. Membr. Sci.* **2010**, *353*, 85–93. [CrossRef]
18. Yadav, A.; Labhasetwar, P.K.; Shahi, V.K. Membrane distillation using low-grade energy for desalination: A review. *J. Environ. Chem. Eng.* **2021**, *9*, 105818. [CrossRef]
19. Stover, R.L. Seawater reverse osmosis with isobaric energy recovery devices. *Desalination* **2007**, *203*, 168–175. [CrossRef]
20. Hauge, L.J. The pressure exchanger—A key to substantial lower desalination cost. *Desalination* **1995**, *102*, 219–223. [CrossRef]
21. Guan, G.; Yang, X.; Wang, R.; Field, R.; Fane, A.G. Evaluation of hollow fiber-based direct contact and vacuum membrane distillation systems using aspen process simulation. *J. Membr. Sci.* **2014**, *464*, 127–139. [CrossRef]
22. Kim, J.; Park, M.; Snyder, S.A.; Kim, J.H. Reverse osmosis (RO) and pressure retarded osmosis (PRO) hybrid processes: Model-based scenario study. *Desalination* **2013**, *322*, 121–130. [CrossRef]
23. Park, Y.; Chung, K.; Yeo, I.; Lee, W.; Park, T. Development of a SWRO-PRO hybrid desalination system: Pilot plant investigations. *Water Sci. Technol. Water Supply* **2018**, *18*, 473–481. [CrossRef]

24. Mericq, J.-P.; Laborie, S.; Cabassud, C. Vacuum membrane distillation of seawater reverse osmosis brines. *Water Res.* **2010**, *44*, 5260–5273. [CrossRef] [PubMed]
25. Kim, J.; Park, M.; Shon, H.K.; Kim, J.H. Performance analysis of reverse osmosis, membrane distillation, and pressure-retarded osmosis hybrid processes. *Desalination* **2016**, *380*, 85–92. [CrossRef]
26. Prante, J.L.; Ruskowitz, J.A.; Childress, A.E.; Achilli, A. RO-PRO desalination: An integrated low-energy approach to seawater desalination. *Appl. Energy* **2014**, *120*, 104–114. [CrossRef]
27. Wan, C.F.; Chung, T.-S. Energy recovery by pressure retarded osmosis (PRO) in SWRO–PRO integrated processes. *Appl. Energy* **2016**, *162*, 687–698. [CrossRef]
28. Ruiz-García, A.; Nuez, I. Performance Assessment of SWRO Spiral-Wound Membrane Modules with Different Feed Spacer Dimensions. *Processes* **2020**, *8*, 692. [CrossRef]
29. Glueckstern, P.; Priel, M. Comparative cost of UF vs conventional pretreatment for SWRO systems. *Int. Desalination Water Reuse Q.* **2003**, *13*, 34–39.
30. Karnland, O. *Bentonite Swelling Pressure in Strong NaCl Solutions. Correlation between Model Calculations and Experimentally Determined Data*; Swedish Nuclear Fuel and Waste Management Co.: Solna, Sweden, 1997.
31. Lee, K.; Baker, R.; Lonsdale, H. Membranes for power generation by pressure-retarded osmosis. *J. Membr. Sci.* **1981**, *8*, 141–171. [CrossRef]
32. Wan, C.F.; Yang, T.; Gai, W.; De Lee, Y.; Chung, T.-S. Thin-film composite hollow fiber membrane with inorganic salt additives for high mechanical strength and high power density for pressure-retarded osmosis. *J. Membr. Sci.* **2018**, *555*, 388–397. [CrossRef]
33. Guillen-Burrieza, E.; Servi, A.; Lalia, B.S.; Arafat, H.A. Membrane structure and surface morphology impact on the wetting of MD membranes. *J. Membr. Sci.* **2015**, *483*, 94–103. [CrossRef]
34. Achilli, A.; Prante, J.L.; Hancock, N.T.; Maxwell, E.B.; Childress, A.E. Experimental results from RO-PRO: A next generation system for low-energy desalination. *Environ. Sci. Technol.* **2014**, *48*, 6437–6443. [CrossRef]
35. Lee, S.; Choi, J.; Park, Y.-G.; Shon, H.; Ahn, C.H.; Kim, S.-H. Hybrid desalination processes for beneficial use of reverse osmosis brine: Current status and future prospects. *Desalination* **2019**, *454*, 104–111. [CrossRef]